

Historical shrub–grass transitions in the northern Chihuahuan Desert: modeling the effects of shifting rainfall seasonality and event size over a landscape gradient

QIONG GAO* and JAMES F. REYNOLDS†

*MOE Key Laboratory of Environmental Change and Natural Disasters, Institute of Resources Science, Beijing Normal University, Beijing 100875, P. R. China, †Department of Biology and Nicholas School of the Environment and Earth Sciences, Box 90340, Duke University, Durham, NC 27708, USA

Abstract

We use a spatially explicit landscape model to investigate the potential role of rainfall on shrub–grass transitions in the Jornada Basin of southern New Mexico during the past century. In long-term simulations (1915–1998) along a 2700 m transect running from a dry lake bed to the foothills of a small mountain, we test two hypotheses: (i) that wetter winters and drier summers may have facilitated shrub encroachment in grasslands, and (ii) that increases in large precipitation events may have increased soil water recharge at deeper layers, thus favoring shrub establishment and growth. Our model simulations generally support the hypothesis that wetter winters and drier summers may have played a key role, but we are unable to reproduce the major shifts from grass- to shrub-domination that occurred in this landscape during the early part of the 1900s; furthermore, the positive shrub response to wetter winters and drier summers was only realized subsequent to the drought of 1951–1956, which was a relatively short ‘window of opportunity’ for increased shrub establishment and growth. Our simulations also generally support the hypothesis that an increase in the number of large precipitation events may also have favored shrub establishment and growth, although these results are equivocal, depending upon what constitutes a ‘large’ event and the timing of such events. We found complex interactions among (i) the amount/seasonality of rainfall, (ii) its redistribution in the landscape via run-on and runoff, (iii) the depth of the soil water recharge, and (iv) subsequent water availability for the growth and reproduction of shrubs vs. herbaceous plants at various landscape positions. Our results suggest that only a mechanistic understanding of these interactions, plus the role of domestic cattle grazing, will enable us to elucidate fully the relative importance of biotic vs. abiotic factors in vegetation dynamics in this semiarid landscape.

Keywords: *Bouteloua*, desertification, hydrology, *Larrea*, *Prosopis*

Received 10 May 2002; revised version received 8 April 2003 and accepted 28 June 2003

Introduction

Ecosystems of the Jornada Basin in southern New Mexico have been dramatically altered in the past century as a result of the extensive encroachment of C3 shrubs – mainly creosotebush (*Larrea tridentata*) and mesquite (*Prosopis glandulosa*) – into C4 grasslands

previously dominated by black grama grass (*Bouteloua eriopoda*) (Buffington & Herbel, 1965; York & Dick-Peddie, 1969). Similar dynamics have occurred throughout the southwestern United States (Grover & Musick, 1990; Bahre & Shelton, 1993; McPherson, 1997; Archer, 1999) and in many other regions of the globe (Reynolds, 2001). The ecological consequences of these changes in terms of primary productivity, nutrient cycling, and water flux are considerable and have important social and economic implications (Reynolds & Stafford Smith, 2002).

Correspondence: Qiong Gao, fax +86(10)6220-6050, e-mail: gaoq@bnu.edu.cn or qgao@duke.edu

Shrub encroachment in the southwest United States in particular has been attributed to various potential causal factors, including overgrazing by domestic cattle, fire suppression, a proliferation of rodents (due to the human elimination of natural predators), climate change, and rising atmospheric CO₂ concentrations (see reviews in Grover & Musick, 1990; Schlesinger *et al.*, 1990; Reynolds *et al.*, 1997). Several hypotheses regarding the role of precipitation in grass–shrub transitions have been proposed. In the Jornada Basin, which is located in the northern portion of the Chihuahuan Desert and is a summer-dominated rainfall system where ca. 65% of the total annual precipitation (230 mm) falls between June and September, Neilson (1986) hypothesized that winter rain was critically important for the establishment of perennial shrubs and that changes in the patterns of winter precipitation since the mid-1850s may have played a role in the historical transition from grass- to shrub-domination. Neilson argued that wet winters provided suitable conditions for the establishment of cool season species (C3 shrubs), whereas wet summers favored the establishment of warm season species (C4 grasses). This hypothesis is supported by Brown *et al.* (1997), who report a three-fold increase in the shrub density since 1970 at three sites in southern Arizona, coinciding with a recent shift (since 1977) in the regional climate in which the winter precipitation was substantially higher than the previous 100-year average.

Another potential key factor is the size of rainfall events. Light rains effectively recharge the upper layers of the soil profile, thus favoring shallow-rooted plants such as grasses, whereas large rain events, in addition to producing more runoff, are crucial for recharging deep soil layers, which is essential for the survival of deep-rooted plants such as shrubs. The role of the surface vs. deep layer water availability and its impact on the coexistence of plant life forms in savannahs was originally proposed by Walter (1971) as the ‘two-layer’ hypothesis. This hypothesis has been both supported and, in several instances, refuted by a large number of studies (see Reynolds *et al.*, 2000b; Schwinning & Ehleringer, 2001).

In this paper, we use a landscape simulation model to investigate the potential role of rainfall on shrub–grass transitions in the Jornada Basin during the past century. Specifically, we test two hypotheses regarding the partitioning of annual rainfall: (i) that wetter winters facilitated shrub invasion into grasslands (Neilson, 1986), and (ii) that an increase in large precipitation events – at the expense of smaller ones – resulted in an increased soil water recharge at deeper layers, which favored the shrub establishment and growth (Walter, 1971). Although the model is formulated and para-

meterized for southern New Mexico, we suggest that this simulation exercise may provide helpful insights for an increased understanding of the potential factors affecting long-term vegetation dynamics in other semiarid regions of the world.

Materials and methods

Site description and climate

Vegetation, weather, and soils data used for the model development and simulations reported in this paper were collected from a 2700 m transect established in 1982 as part of the Jornada Basin Long Term Ecological Research (LTER) site, which is located in a semiarid rangeland of south-central New Mexico about 40 km NNE of Las Cruces, NM. The 30 m wide transect consists of 90 sampling stations located 30 m apart on an alluvial fan, extending southwest from a dry lake bed (playa) to the foothills of Mt Summerford, an increase in elevation of approximately 100 m (Fig. 1). Detailed descriptions of vegetation and soils along the transect are provided in Wierenga *et al.* (1987), Cornelius *et al.* (1991), and Kemp *et al.* (2003a).

The climate of the Jornada Basin is characterized by three distinct seasons: hot, dry springs (April–June); hot, moist summers (July–October); and cold, moderately dry winters (November–March) (Conley *et al.*, 1992). The annual mean temperature is 14.4 °C, with 26.0 °C and 3.5 °C as the mean temperatures in June and December, respectively. The mean annual precipitation is 230 mm, with a large interannual variation from 140 to 532 mm. About 65% of the total precipitation occurs in brief, local, but relatively intense, convective thunderstorms from June to September. In this paper, the period from October 1 to May 31 is designated ‘winter/spring’ and the period from June 1 to September 30 as ‘summer’. Rainfall and temperature from the USDA Jornada Experimental Range, from April 1, 1915 to March 31, 1998, were used for the long-term simulations (available at <http://jornada.nmsu.edu>).

Plant functional types

Our modeling at this site is based on the use of plant functional types (FT) or life forms (Reynolds *et al.*, 1997), including annuals (winter- or summer-active species), perennial forbs (species active from spring through autumn), grasses (all are C4, summer-active species, e.g., black grama, *B. eriopoda*), sub-shrubs (primarily winter deciduous; *Xanthocephalum* and *Zinnia* spp.), deciduous shrubs (primarily mesquite, *P. glandulosa*), and evergreen shrubs (primarily creosotebush, *L. tridentata*). For simplicity, in this paper we

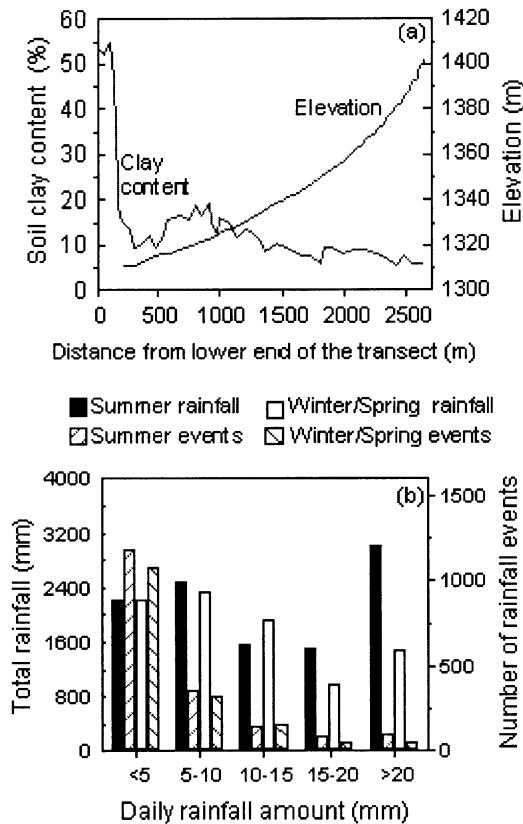


Fig. 1 (a) Soil clay contents and elevation profile of the LTER transect, which runs from a small dry lake bed (playa, lower end) to the foothills of Mt Summerford (redrawn from Wierenga *et al.*, 1987). (b) Daily rainfall statistics covering the 83-year period from April 1, 1915 to March 31, 1998 at the Jornada Experimental Range. Winter/spring covers the period from October 1 to May 31, whereas summer is from June 1 to September 30.

limit our analysis to three FTs: evergreen shrubs (i.e., *Larrea*), deciduous shrubs (i.e., *Prosopis*), and ‘grass + herbs’ (a category dominated by *Bouteloua*, but including all herbaceous plants). These FTs are representative of the dominant plant communities involved in the documented grass–shrub transition that occurred in this region during the past century, and we assume that the different combinations of FTs along the transect are representative of the different stages in this transition (Reynolds *et al.*, 2000b). For example, currently station 80 is dominated by grasses (representative of vegetation ca. 1930), whereas station 65 is dominated by *Larrea* (ca. 1970).

From 1982 to 1987, biannual (early spring and late fall) measurements on plant cover were made at each station. Using allometric relationships, we converted these cover data into leaf and stem aboveground biomass and leaf area index. These fall data, which represent the peak, growing season cover, are used here

for model validation; the spring data are highly variable and are used only to estimate initial biomass for FTs (see below). In addition, the volumetric soil water content was measured about every 2 weeks at five depths (from 30 to 120 cm) at each station along the transect. The complete details of the plant and soil water sampling protocols and data analyses for the transect are provided in Cornelius *et al.* (1991) and Kemp *et al.* (1997).

Model description

Previously, we have used the patch arid land simulator (PALS) to explore the potential effects of rainfall variability on carbon–nitrogen dynamics in the Jornada Basin. PALS is an ecosystem model that consists of a coupled set of modules of soil water, decomposition, energy-budget/atmospheric environment, and the physiology and phenology of the principal FTs found in the arid zones of the southwestern United States. To date, PALS has been applied to investigate hypotheses concerning abiotic vs. biotic controls on primary production (Reynolds *et al.*, 1997; Reynolds *et al.*, 2000a; Ogle & Reynolds, 2002), decomposition and soil nutrient cycling (Kemp *et al.*, 2003b), and plant–soil water dynamics (Kemp *et al.*, 1997; Reynolds *et al.*, 2000b).

Although PALS has been tested under a range of environmental conditions, it is restricted to small-scale, homogeneous patches, and consequently is unable to account for important spatial phenomena that may affect shrub–grass transitions in semiarid regions, e.g., seed dispersal (Wiegand *et al.*, 1995) and hydrologic runoff and run-on (McAuliffe, 1988; Wainwright *et al.*, 1999). In this paper, we present the mosaic arid land simulator (MALS), a spatially explicit adaptation of PALS, which overcomes these limitations. A brief description of MALS is provided in Appendix A. The model has an integration time step of 1 day, a spatial resolution of 10 × 30 m, and is designed to be driven by daily weather, including rainfall, temperature (maximum, minimum, and mean), humidity, wind speed, and solar radiation.

Model implementation and parameterization

To implement MALS, the 2700 m LTER I transect (Fig. 1) was divided into 270 contiguous grid cells, each 10 m long × 30 m wide. The cell at the lower end of the transect (playa) is designated the ‘lower end’ of the transect throughout the text. The grid cells are numbered from 1 (lower end) to 270 (upper). Geometric symmetry in the direction perpendicular to the transect is assumed; i.e., there is no net mass and energy exchange at the side boundaries. Each cell receives

run-on from adjacent uphill cells and loses runoff to adjacent downslope cells (see Eqn (A.14), Appendix A). The upper end of the transect receives runoff from the foothills of Mt Summerford, which is assumed to be proportional to the total rainfall amount, and the proportionality constant is adjusted so that the soil water content (averaged over space and time in the simulation range) is approximately equal to the field observations in the 1980s. The lower end of the transect discharges surface runoff into the playa. We do not consider lateral, subsurface flows. A total of 13 parameters (i.e., Y in Eqn (A2), d_{root} in Eqn (A11), d_{stem} and d_{leaf} in Eqn (A12) for each of the three FTs, and the proportionality of the runoff input in the upper end of the transect) were adjusted to fit the data.

Details of the parameterization of the soil water module, including the algorithm used for setting the rooting depths of the plant FTs, are provided in Kemp *et al.* (1997). Physiological parameters for the grass + herbs and evergreen plant FTs are from Reynolds *et al.* (2000b); for the deciduous shrub FT, they are based on previous modeling (Reynolds *et al.*, 1997) and our field data (de Soyza *et al.*, 1996; Reynolds *et al.*, 1999). The seed dispersal parameters are based on the field observations of Guo *et al.* (1998), whereas seed germination and seedling survival of the shrub FTs have been estimated from the literature (e.g., Barbour, 1968; Bush & Van Auken, 1987; Bush & Van Auken, 1990; Bush & Van Auken, 1991). Rhizome propagation for the grass + herbs FT follows the approach in Gao *et al.* (1996). No net seed and rhizome movement across the boundaries of the transect is assumed.

Short-term validation

To provide an independent assessment of the model's behavior, we compare the observed peak cover/biomass and soil water data from the LTER transect with the model's output over a 5-year period. Coinciding with the period of data collection, MALS was run for 5 years (April 1, 1983 to October 1, 1987) using records from the Jornada LTER weather station. To initialize MALS, we use the leaf and stem biomass for the plant FTs and soil water contents observed at 30 and 60 cm depths in the early spring of 1983; the seed biomass for all FTs was assumed to be zero, and the initial root biomass was estimated from observed root:shoot ratios (Reynolds *et al.*, 1999).

Long-term scenarios

For the long-term (decadal) simulations, we used daily rainfall and temperature data from April 1, 1915 to March 31, 1998 obtained from the nearby USDA

Jornada Experimental Range weather station. The summary statistics of these data are shown in Fig. 1b. The wind speed, relative humidity, and solar radiation were generated from the statistical relationships between these quantities and rainfall and temperature derived from the Jornada LTER weather data.

To test the two hypotheses, daily rainfall was manipulated as follows:

- (1) *Shifting rainfall seasonality (four scenarios)*: To test whether wetter winters and drier summers may have facilitated shrub invasion into the grasslands, the amount of daily rainfall from October 1 to May 31 (winter/spring) was increased by 0%, 20%, 40%, and 60%, while rainfall from June 1 to September 30 (summer) was decreased accordingly, so that the total rainfall each year was preserved.
- (2) *Adjusting rainfall event sizes (four scenarios)*: To test whether an increase in the number of large precipitation events could result in an increased soil water recharge at deeper layers, rainfall events of amounts less than 5, 10, 15, and 20 mm in each of the two seasons (winter/spring and summer) were successively removed from the 83-year observed rainfall sequence for the Jornada Basin. These 'removed' events were added back to the remaining larger-sized events to preserve total annual amounts and the ratios of summer to winter/spring precipitation. In sum, these scenarios 'redistribute' the annual rainfall into larger-size events (Fig. 1b). Several of these scenarios are illustrated in Fig. 2.

For each of the eight scenarios – run from April 1, 1915 to March 31, 1998 (83 years) – the same boundary conditions, initial soil water contents, and the spatial and temporal resolution were used as in the short-term validation described above. Given that we are interested in the potential transitions from a grass- to shrub-dominated system after 83 years, we used the following initial conditions. For the grass + herbs FT, root, stem, and leaf biomass in all grid cells were set to 10, 10, and 10 g m^{-2} , respectively, whereas for *Larrea* and *Prosopis*, they were set to 0, 0, and 0 g m^{-2} , with the following exception: for *Prosopis* at grid cell 20 and for *Larrea* at grid cell 250, these values were initialized at 100, 200, and 300 g m^{-2} , respectively.

Runoff/run-on redistribution scenarios

The topographic position, and the generation of runoff and run-on, has the potential to exert a major influence on the eco-hydrology of semiarid systems. To examine this for the transect, we implement two versions of

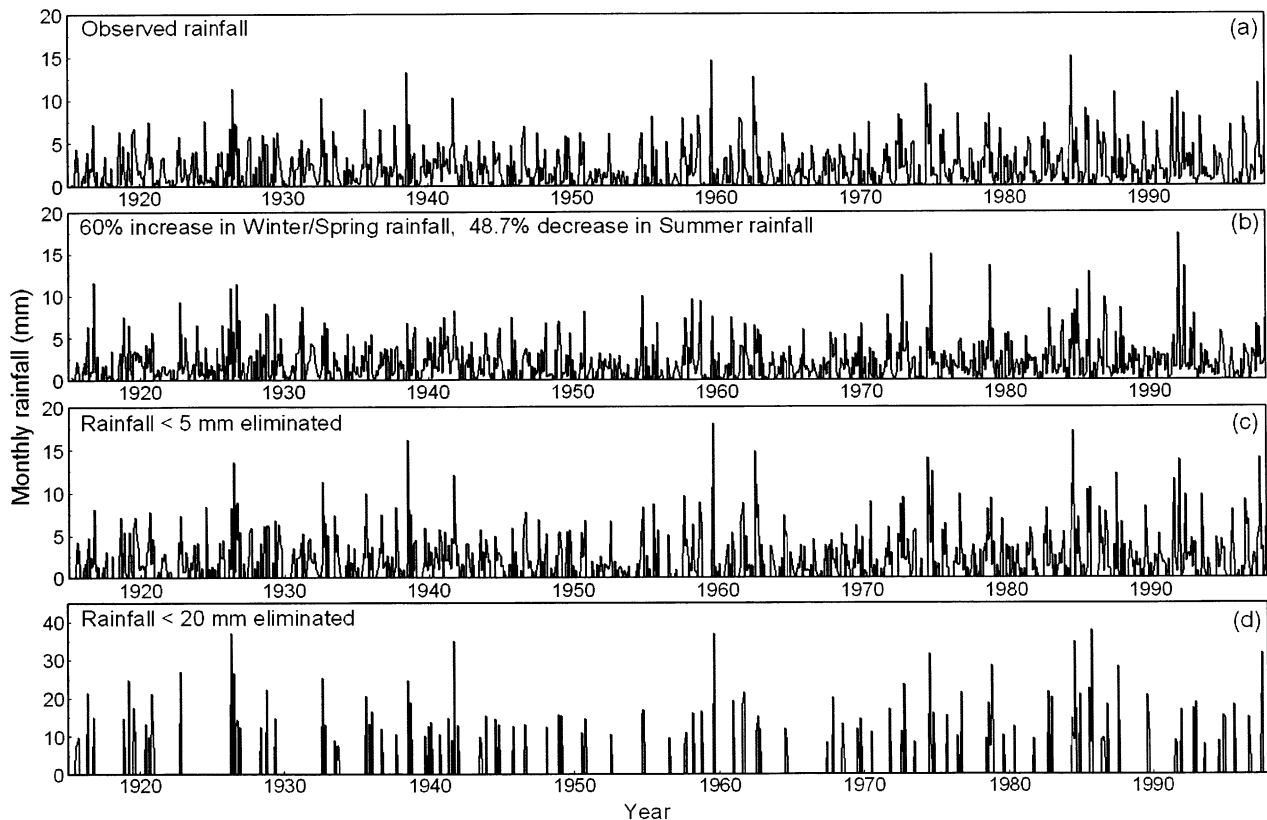


Fig. 2 (a) Observed monthly rainfall scenarios (1915–1998) from USDA Jornada Experimental Range; (b) simulated 60% increase in winter/spring rain with subsequent 48.7% decrease in summer rainfall; (c) daily rainfall events < 5 mm removed from time series; and (d) daily rainfall events < 10 mm removed from time series.

MALS: one *with* and the other *without* runoff/run-on redistribution (see Section A.5, Appendix A). In the version without runoff/run-on redistribution, the runoff produced at an individual grid cell (i.e., when precipitation > infiltration) is removed from the system.

Results and discussion

Short-term evaluation of the model

In Fig. 3, the simulated leaf and stem biomass of the three plant FTs are compared with the 5 years of observations of the fall, peak-season standing biomass along the transect. We found no significant differences in the observed vs. model predictions based on a paired *t*-test ($n = 449$) of mean differences: grass + herbs ($t_{\text{leaf}} = 0.438$; $t_{\text{stem}} = 1.252$), *Larrea* ($t_{\text{leaf}} = 0.302$; $t_{\text{stem}} = 0.301$), and *Prosopis* ($t_{\text{leaf}} = 0.303$; $t_{\text{stem}} = 0.017$). The year-to-year variability in the modeled production is relatively high, both between years as well as spatially along the transect. The grass + herbs FT exhibits the highest variation whereas the shrubs FT less so. These results are consistent with the observations of these plant FTs

at a variety of adjacent sites in the Jornada Basin (e.g., Huenneke *et al.*, 2002; Kemp *et al.*, 2003a).

The simulated and observed volumetric water contents in the middle (15–40 cm) and bottom (40–80 cm) soil layers along the transect are shown for select days in June and August of each year in Fig. 5a and b, respectively. The model does a good job of tracking the spatial and temporal dynamics of soil water during the 5-year period. The root mean square error (RMSE) between the simulated and observed soil water contents is 16.21 for the middle layer ($n = 7974$) and 17.04 for the bottom layer ($n = 7990$). Combining the residual and total sums of squares and the number of parameters, we obtain statistically significant *F*-values of $F_{7962}^{13} = 4639$ for the middle layer and $F_{7978}^{13} = 4489$ for the bottom layer ($F_{\infty}^{13}[P < 0.01] = 2.12$). The model explains 85.7% and 85.2% of the variation in water contents in the middle and bottom soil layers, respectively. A summary of the observed vs. predicted values is given in Fig. 4.

In our previous efforts to model the soil water dynamics along the transect using the PALS model, we were unable to capture satisfactorily the soil water

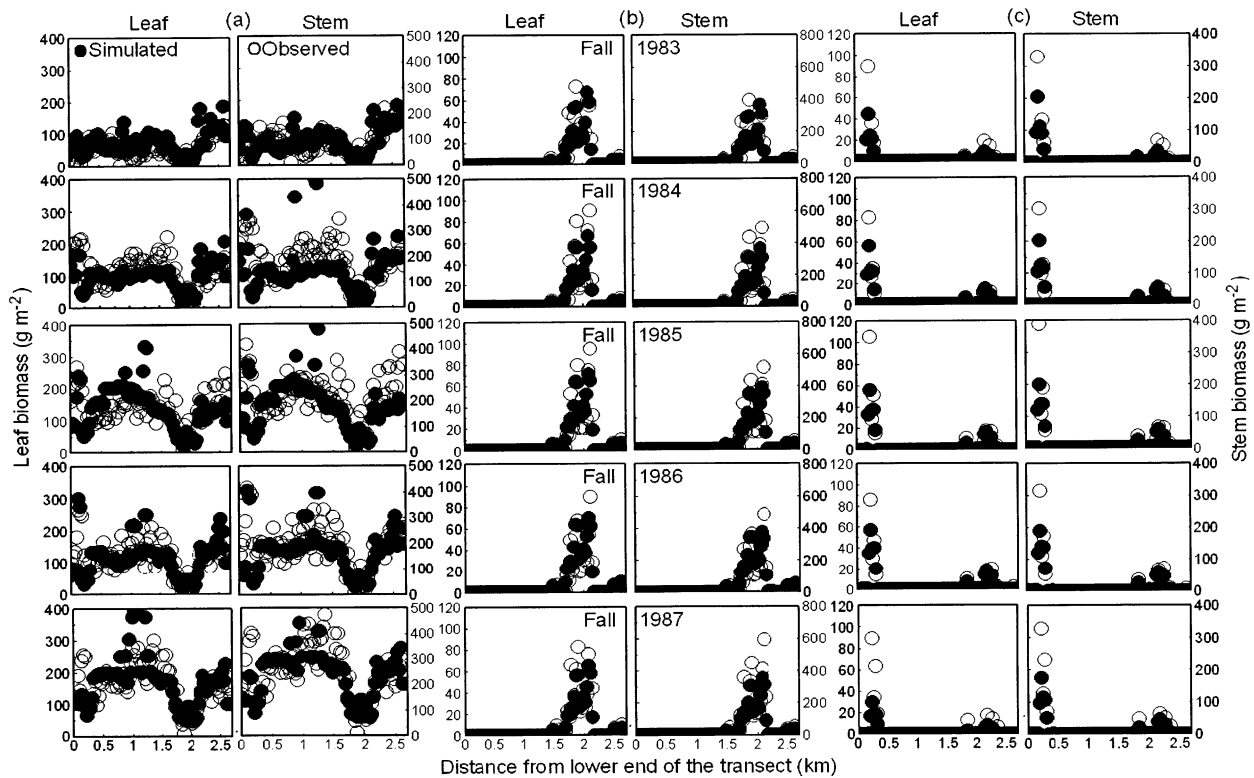


Fig. 3 Comparison of the simulated (closed circles) and observed (open circles) leaf (left column) and stem (right column) peak standing biomass for the plant FTs at the 90 stations along the 2700 m transect from the fall of 1983 to 1987: (a) grass + herbs; (b) evergreen shrubs (i.e., *Larrea*); (c) deciduous shrubs (i.e., *Prosopis*).

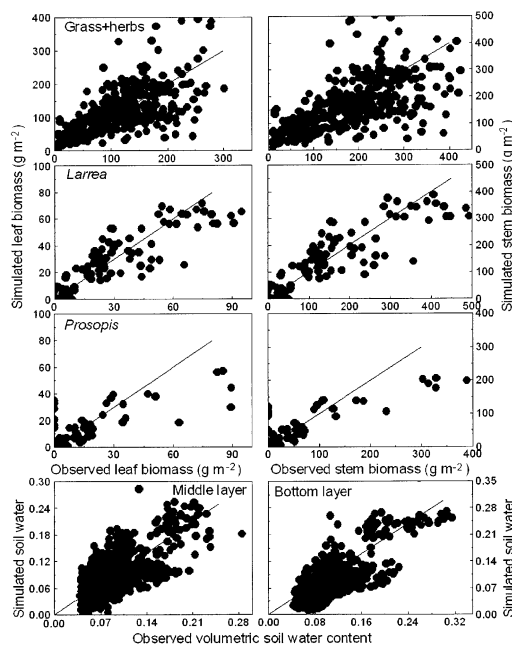


Fig. 4 Simulated and observed peak standing biomass (leaf and stem) for the plant FTs and soil water content at the middle (15–40 cm) and bottom (40–80 cm) layer. Results are pooled from the 90 stations along the 2700 m transect, from the fall of 1983 through 1987.

recharge at 30 and 60 cm depths at the end of the summer growing season (Kemp *et al.*, 1997). Since most rainfall during this period produces some runoff from these basin slopes, we concluded that this was, in part, possibly related to run-on and runoff (which are not considered in PALS). This conclusion is supported by our results with MALS, which does a good job of late season (August) soil water recharge at both medium and deeper soil depths (Fig. 5).

Seasonality scenarios – observed rainfall

The results of the long-term scenarios are presented in Figs 6–8. First we discuss the observed rainfall scenario; next, we discuss the effects of shifting rainfall from the summer to the winter season.

The year-to-year variability in production in the grass + herbs FT reflects the relatively strong dependence on the total annual rainfall. As in the previous modeling efforts at this site (e.g., Reynolds *et al.*, 2000b), the variability of this relationship is very high. The reasons underlying this variability are numerous, as illustrated by the ‘wet’ decade from 1984 to 1993. As compared with the 100-year mean for the site, there is a

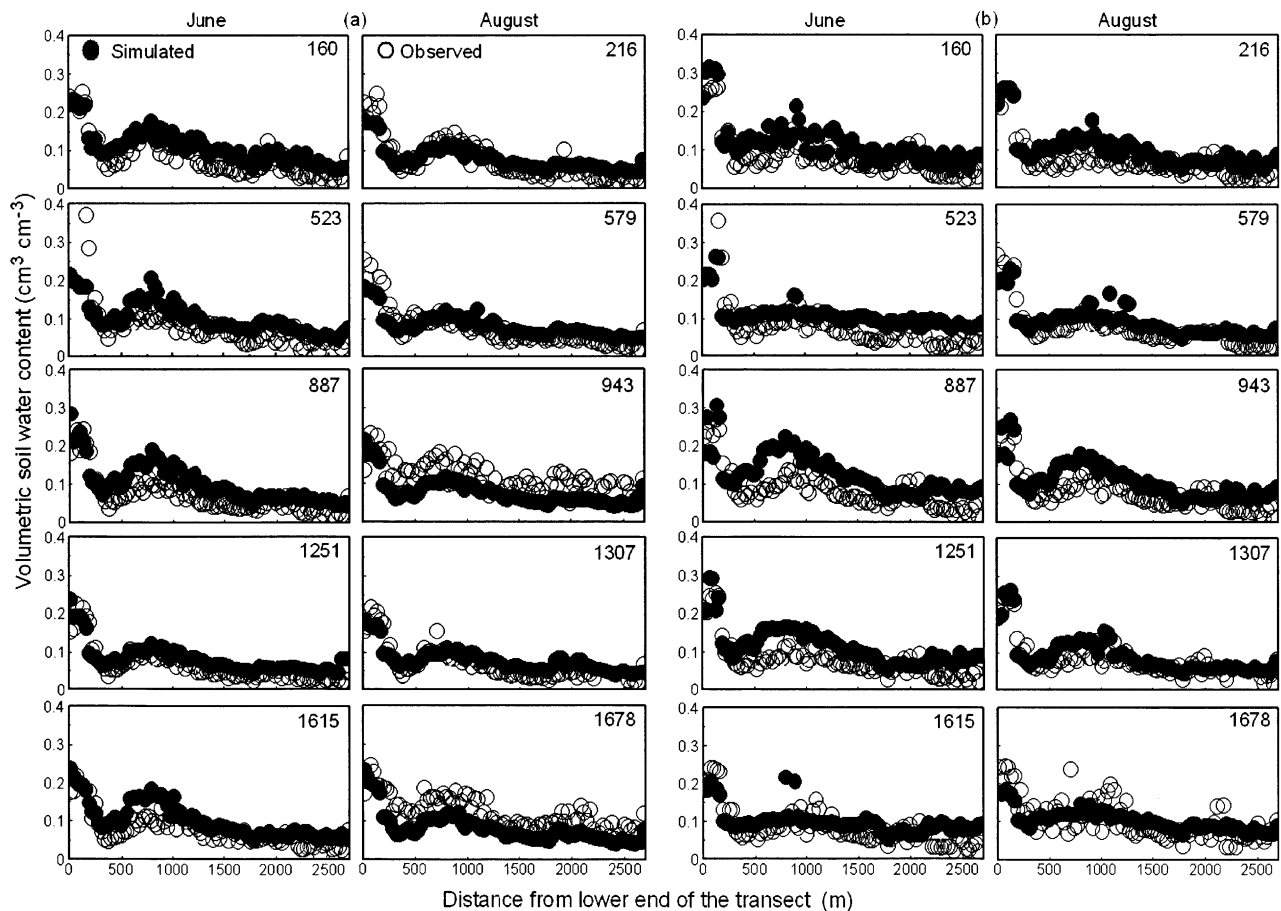


Fig. 5 Comparison of simulated (closed circles) and observed (open circles) volumetric soil water content ($\text{cm}^3 \text{cm}^{-3}$) of the (a) middle soil layer (15–40 cm depth) and (b) bottom soil layer (40–80 cm depth) at the 90 stations along the transect during the 5-year period. Only the values for early June (i.e., Julian days 160, 523, 887, 1251, and 1616 for 1983–1987, respectively; left columns) and early August (right columns) are shown.

slightly increased summer rainfall (10%), a greatly increased spring (April–June) rainfall (85%), and a greatly increased winter rainfall (50%) (see Reynolds *et al.*, 2000b). However, during this ‘wet’ decade, the grass + herbs FT has a large, positive growth response (Fig. 6a). This is somewhat counterintuitive since most of the growth of this FT normally occurs in the summer, yet summer rainfall increased by only 10%. We explain this by noting that while grasses break dormancy in spring as the average temperature climbs above 10°C , growth in the next three months is usually minimal (normally a very dry period in the northern Chihuahuan Desert – Conley *et al.*, 1992), and hence the unusually wet spring period during this particular decade may have provided a ‘head start’ in growth leading into the summer months. This conclusion is supported by Fernández & Reynolds (2000), who note that the length of the spring drought period is related to the C4 grass growth in the summer because the death of

the root and shoot tissue reduces the number of growing points capable of utilizing the summer rainfall.

These dynamics can be contrasted with those during the drought of 1951–1956, which is embedded within a generally dry period from 1942 to 1956 (Swetnam & Betancourt, 1998). Here, the grass + herbs FT biomass declines substantially (Fig. 6a), consistent with the findings of Gibbens & Beck (1988), who reported that the aboveground cover of the principal range grasses of the Jornada Basin was severely impacted by this drought.

The simulated aboveground biomasses of the two shrub FTs during the 83-year period of simulation are shown in Fig. 7. When using observed rain to drive the model, the biomass of both shrub FTs remains at a low, constant level until the mid-1950s (solid lines, Fig. 7). Whereas the 1942–1956 dry period generally has a negative impact on the growth of the shrub FTs, thereafter both undergo increased (albeit slow) rates

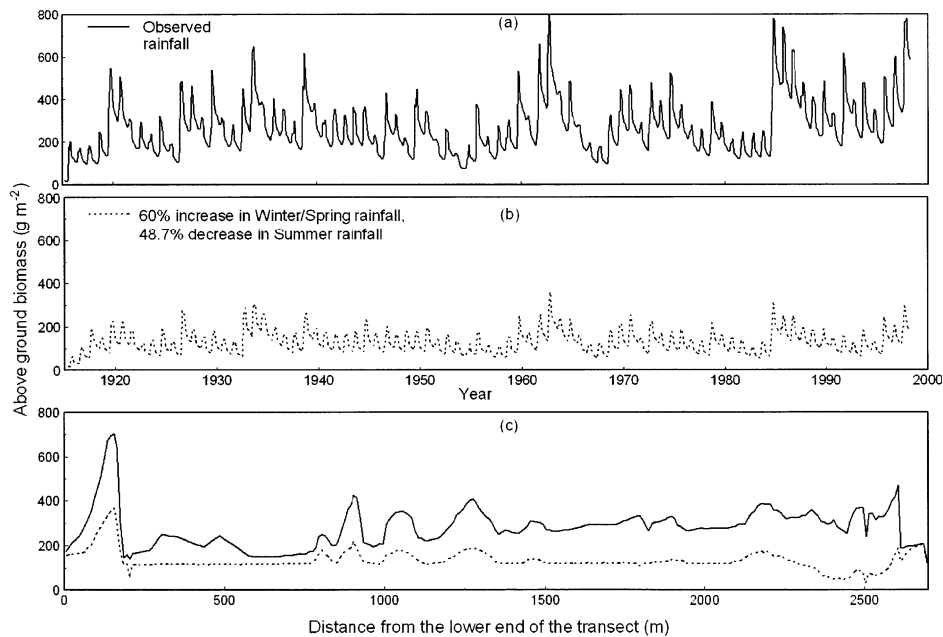


Fig. 6 (a, b) Spatially averaged $(\frac{1}{270} \sum_{x=1}^{270} m_a^i(t_m, x))$ and (c) temporally averaged $(\frac{1}{996} \sum_{t_m=1}^{996} m_a^i(t_m, x))$ grass + herbs aboveground biomass with observed rainfall (solid line) and 60% increase in the winter/spring rainfall at the expense of a 48.7% decrease in the summer rainfall (dashed line), where t_m is the time (month), x is the grid number along the transect, and $m_a^i(t_m, x)$ is the aboveground biomass for FT i at time t_m at grid cell x . Note: the total annual rainfall is the same for both the scenarios and results for the version with the runoff/run-on redistribution only are shown.

of growth, establishment, and proliferation (*Larrea* is restricted to the upper end of the transect and *Prosopis* to the lower end). *Prosopis* generally has a similar response to *Larrea*, but the absolute values of biomass at the end of the simulation period are substantially smaller than the present-day values along the transect (Fig. 3b, also see Kemp *et al.*, 2003a). This underestimation is likely related to several assumptions in this version of the model, especially the lack of soil nutrient feedbacks. Seasonal shifts in nutrient feedbacks were found to be important by Epstein *et al.* (1999) in a modeling exercise in semiarid short-grass steppe, where precipitation was switched from summer to spring, as was found by Reynolds *et al.* (1999) in a field manipulation of the winter and summer rainfall in the Jornada Basin, and by Kemp *et al.* (2003b) when modeling these dynamics. This is due to the complex interactions between precipitation, soil organic matter, nutrient availability, and plant growth.

Seasonality scenarios – shifting to winter rainfall

The effects of shifting rainfall from the summer season (June 1 to September 30) to the rest of the year (October 1 to May 31) on soil water and aboveground biomass are summarized in Fig. 8 using a synthetic average. This synthetic average represents an approximate

integration of the area under the curves (solid vs. dashed) in Figs 6 and 7, computed over the entire length of the transect and the 83-year time series.

Shifting rainfall from the summer to winter seasons affects all plant FTs, and these effects are always larger when runoff/run-on redistribution is considered (see below). Across the entire range of shifts considered (i.e., 0–60%), the following results are evident: (i) Soil water content, averaged across the three soil depths, increases about 12% (10% when run-on is excluded; Fig. 8d). This increase is due, at least in part, to a decrease in evapotranspiration, which is smaller in the winter–spring period than in the summer (analysis not shown). (ii) The aboveground biomass of the grass + herbs FT decreases 44% (37% without run-on; Fig. 8a). (iii) The aboveground biomass for both the shrub FTs increases, about 6 × for *Larrea* (Fig. 8b) and 3 × for *Prosopis* (Fig. 8c). As is evident in Fig. 7 (dashed vs. solid lines), these increases reflect the increasing spatial distributions of these shrub FTs along the transect.

Gibbens & Beck (1988) speculated that the drought of the 1950s may have favored an increase in shrubs in the Jornada Basin. Indeed, our results show that the grass + herbs FT is strongly impacted by the drought of the 1950s. However, the subsequent period is mainly one of ‘recovery’ for the grass + herbs FT (Fig. 6a), a pattern consistent with data for a variety of species (but

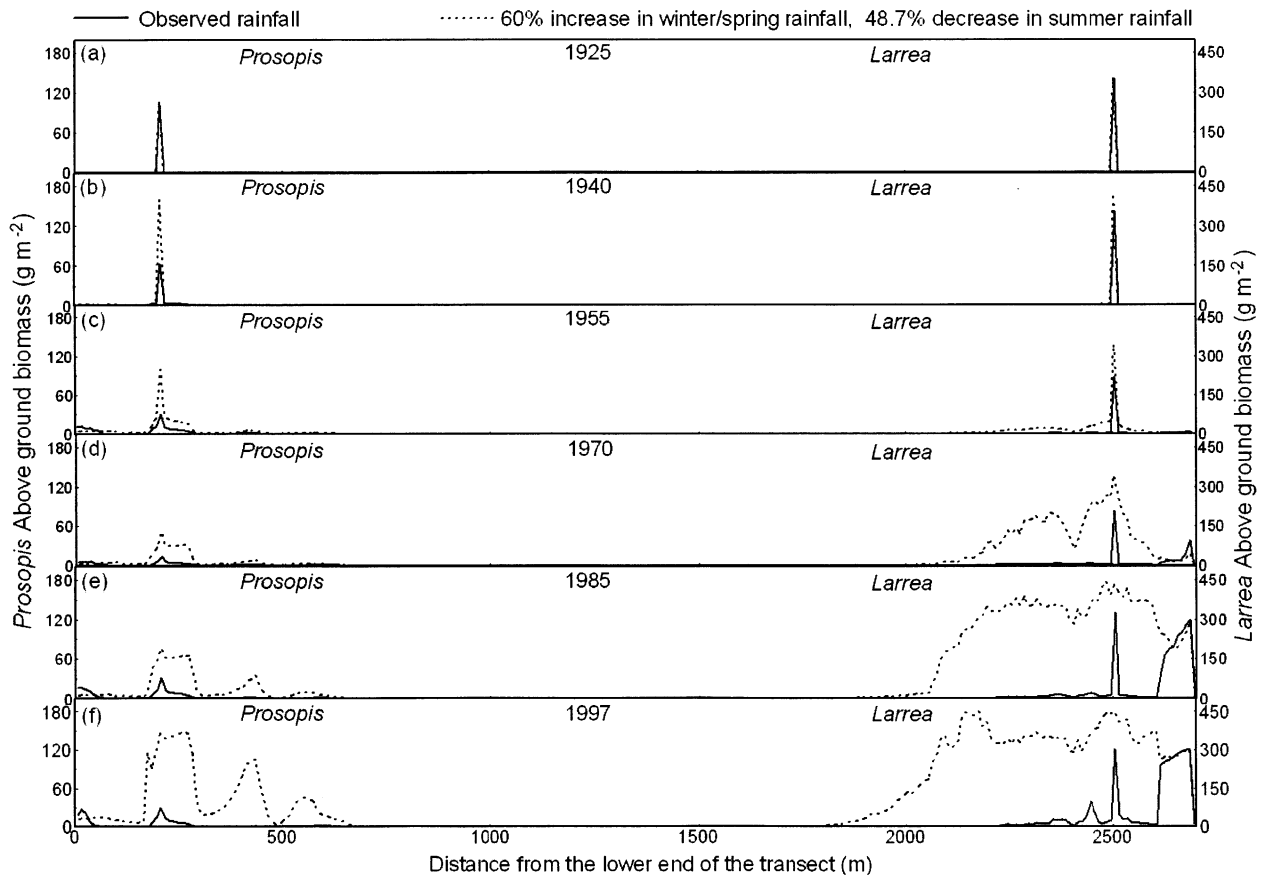


Fig. 7 Simulated aboveground biomass along the 2700m transect for the evergreen and deciduous shrub FTs (*Prosopis* and *Larrea*, respectively). The 15-year periods from 1925 to 1997 (peak values in August) as a function of the observed daily rainfall (solid line) and with a 60% increase in the amount of winter/spring rain (October 1 to May 31) shifted from the summer period (June 1 to September 30) (dashed line) are shown. Note: the total annual rainfall is the same for both the scenarios, and results for the runoff/run-on redistribution version of the model only are shown.

not all, e.g., *B. eriopoda*) in both Gibbens & Beck (1988) and Herbel *et al.* (1970). Thus, while an obvious 'window of opportunity' exists for shrub encroachment – and our simulations with observed rainfall (see the previous section) suggest that shrubs would have been less impacted by the drought of the 1950s than grasses – our results appear to support this supposition *only* if accompanied by increased winter rainfall. Hence, one of our key findings is that an increased growth and expansion of shrubs occurs only when two conditions are simultaneously met: (i) the drought of the 1950s (which serves as a 'window of opportunity' for initiating increased shrub growth and expansion) and (ii) an increase in winter rainfall.

Hence, in the context of elucidating the potential mechanisms involved in historical grass-shrub transitions in the Jornada Basin, our simulation results are somewhat equivocal. First, while our model matches many of the general patterns of grass-shrub dynamics

since the 1950s (documented in Gile *et al.*, 1988), when using observed rainfall to drive the model we fail to reproduce the major shift from grass- to shrub-dominance in the early part of the 1900s (Buffington & Herbel, 1965; York & Dick-Peddie, 1969). Second, Conley *et al.* (1992) and Reynolds & Kemp (unpublished) found no statistical evidence for increased winter rainfall in the Jornada Basin during this critical period (Brown *et al.* (1987) reported increased winter rainfall, but for 1977–1992 only). These findings suggest that other factors not included in this version of MALS, such as grazing by domestic livestock, may be important.

Adjusting rainfall event size scenarios

The effects of redistributing rainfall within a year into larger-size events are summarized in Fig. 9. There are two striking differences as compared to the results

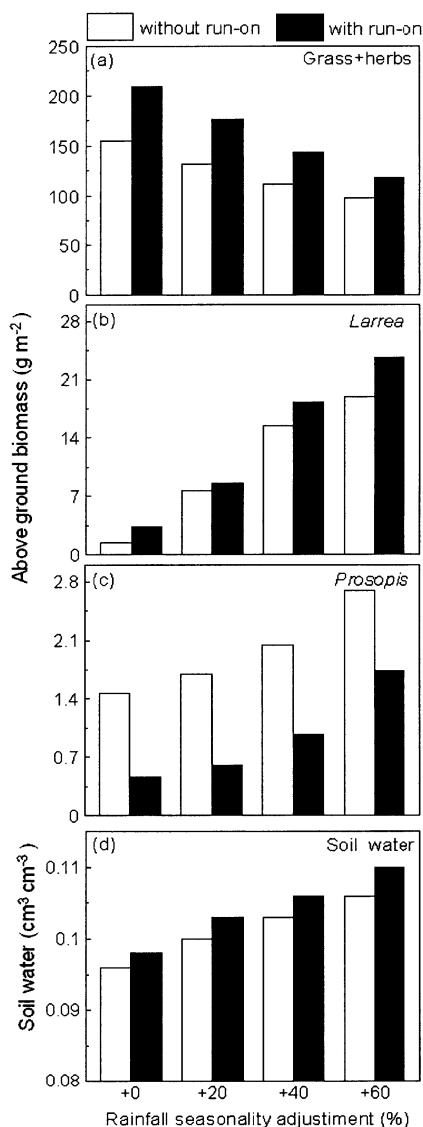


Fig. 8 Synthetic average, proportional to integration of area (biomass) under the curves in Figs 6 and 7, computed over the entire length of the transect and the 83-year time series: $\frac{1}{996 \times 270} \sum_{t_m=1}^{996} \sum_{x=1}^{270} m_a^i(t_m, x)$ for (a) grass + herbs FT, (b) *Larrea*, and (c) *Prosopis*, where t_m is the time (month), x is the grid number along the transect, and $m_a^i(t_m, x)$ is the aboveground biomass for FT i at time t_m at grid cell x . (d) Synthetic average for volumetric soil water content computed as $\frac{1}{996 \times 270 (\Delta Z^1 + \Delta Z^2 + \Delta Z^3)} \sum_{t_m=1}^{996} \sum_{x=1}^{270} [\theta^1(t_m, x) \Delta Z^1 + \theta^2(t_m, x) \Delta Z^2 + \theta^3(t_m, x) \Delta Z^3]$, where $\theta^j(t_m, x)$ and Z^j for $j=1, 2$, and 3 are the volumetric water content and thickness of soil layer j , respectively). The amount of daily rainfall from October 1 to May 31 each year was increased by 0% (observed), 20%, 40%, and 60%, while rainfall from June 1 to September 30 was adjusted accordingly to preserve the total observed annual rainfall. Results for both versions of the model – with and without runoff/run-on redistribution – are illustrated.

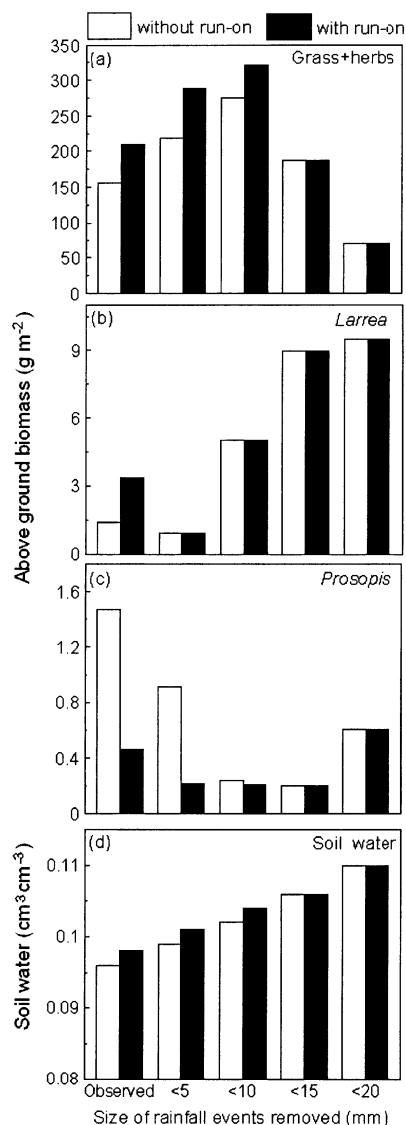


Fig. 9 Synthetic average for aboveground biomass for (a) grass + herbs FT, (b) evergreen shrubs FT (*Larrea*), and (c) deciduous shrubs FT (*Prosopis*); and (d) volumetric soil water content shown in four scenarios that progressively 'redistribute' rainfall into larger-size events while maintaining the total observed rainfall each year and the ratio of summer to winter/spring precipitation. Results for both versions of the model (with and without runoff/run-on redistribution) are illustrated. See Fig. 8 for a description of the synthetic average.

obtained when increasing winter/decreasing summer precipitation (Fig. 8): (i) the nonlinear responses of all three FTs and (ii) the large number of instances where run-on has no effect on the response.

The removal of all precipitation events <10 mm in size has the effect of increasing the biomass of the grass + herbs FT by about 77% (54% with run-on

included) as compared with the observed rainfall; this pattern is dramatically reversed with the removal of successively larger events, decreasing 55% (67% with run-on) when all events <20 mm are removed (Fig. 9a). *Larrea* exhibits a very different response. The removal of the smallest rainfall events (i.e., <5 mm) has the effect of decreasing the average evergreen shrub FT biomass by about 33% (72% with run-on). We are unable to explain this fully, especially since the average soil water content increases (see below) and removing successively larger events significantly increases the biomass (about 2–5 ×; Fig 9b). As compared with the observed rainfall, the biomass of the deciduous shrub *Prosopis* is decreased by all the light rain removal scenarios with the exception of the <20 mm events with run-on only, which results in a slightly increased biomass due to (most likely) competitive interactions with the grass + herbs FT.

The synthetic average of the soil water content (computed over the length of the transect, vertically for three soil layers, and for the 83-year time series) increases linearly with the removal of light rains (Fig. 9d). The effects of including run-on in the model diminishes as successively larger events are removed (up to <20 mm in size). This increase in soil water is a result of the reduction in the surface evaporation associated with the removal of the smaller rainfall events (i.e., 5–10 mm) and a decrease in the overall plant transpiration due to the decrease in grass + herbs FT biomass when the larger (i.e., 15–20 mm) rain events are removed. Since the grass + herbs FT is present along most of the transect, the increase in the shrub biomass with the removal of events <10–20 mm is offset by decreased grass + herbs FT biomass, resulting in less total transpiration loss.

The nonlinearity of responses displayed in Fig. 9 is indicative of the multiple, interacting factors involved in determining the growth and reproduction of plants in arid and semiarid regions. As shown by Reynolds *et al.* (2000b), there are many seasons at the Jornada Basin where substantial rain may not translate into net production, at least for some plant FTs; in other instances, a small amount of rainfall precisely timed such that a particular FT is able to utilize it can result in a large response. Similarly, small events are not necessarily equivalent to the same amount of rain occurring as a single event, which may both produce runoff and percolate deep within the soil profile. Hence, the size of the rain events, and the dry periods between them, affects soil water availability: small or light showers separated by dry periods will result in short growth episodes of adequate soil moisture; if the same amount comes in larger events with higher infiltration, the growth episode will be longer (Burgess, 1995). In the case of the grass + herbs FT, the timing and amount

of individual rain events become much more important in the summer when the C4 grasses are active as compared to the winter. As seen in Fig. 1b, there is roughly twice as much total rainfall that occurs in events >20 mm during the summer months than the rest of the year, yet this occurs in about the same number of total events. In sum, the magnitude of the responses of the plant functional types in this semiarid ecosystem tends to vary, depending upon the previous year as well as current conditions, e.g., successive 'wet' and 'dry' years, as also reported by others (e.g., Golluscio *et al.*, 1998; Reynolds *et al.*, 1999).

Runoff/run-on redistribution scenarios

The strong relationship between the runoff/run-on redistribution and primary production in arid and semiarid ecosystems is well documented (Freudenberger & Hiernaux, 2001). We found the effects of the runoff/run-on redistribution on the responses of the plant FTs and soil water dynamics to be generally significant and, in several instances, dramatic.

In the *shifting rainfall seasonality scenarios* (Fig. 8), the presence of runoff/run-on flows along the transect partially ameliorates the decrease in the grass + herbs FT biomass with shifts to greater winter precipitation. Note that the relative amount of this effect diminishes with a greater shift in rainfall from summer to winter/spring (Fig. 8a) since the grass + herbs FT is mainly summer active. Production in the shrub FTs is also affected by lateral hydrologic flows, but in opposite ways. The runoff/run-on flows result in slight increases in the biomass of *Larrea*, with this effect tending to be relatively more significant with an increasing shift in rainfall away from the summer months (Fig. 8b). In contrast, the runoff/run-on flow actually leads to a decrease in the *Prosopis* biomass by more than 50%, and this reduction does not appear to be influenced by rainfall seasonality (Fig. 8c). Most of the runoff from the upper portion of the transect is locally restricted to within these zones – and utilized by the other plant functional types; hence, for *Prosopis*, which is located near the lower end of the transect, there is a limited amount of lateral flow (results not shown). Overall, there is a small, but significant, increase in the average soil water content when runoff/run-on is included in the model (Fig. 8d).

In the *adjusted rainfall event sizes scenarios* (Fig. 9), the presence of runoff/run-on redistribution is generally much less significant. The patterns of the effect are similar to those described above for shifts in rainfall seasonality, but tend to diminish or completely disappear completely as larger rainfall events are removed. With fewer rainfall events remaining in the

time series (data not shown), the lateral flow is less frequent and hence of reduced importance.

Conclusions

In the context of grass–shrub transitions in the Jornada Basin (northern Chihuahuan Desert) during the past 100 years, we conclude the following:

- (i) Results from our landscape modeling generally support the hypothesis that wetter winters and drier summers could have played a role in shrub encroachment, but with important caveats. Wetter winters and drier summers decreased the grass growth and accelerated the seedling establishment, seedling survival, and growth rates for both the evergreen and deciduous shrub functional types, leading to a significant expansion along the transect. However, we were unable to reproduce the major shifts from grass- to shrub-domination that occurred in the *early part* of the past century and, furthermore, the positive shrub response to wetter winters and drier summers was realized only in the *latter part* of the century following the drought of 1951–1956.
- (ii) The drought of 1951–1956, which was the worst of the century in the southwest United States (Swetnam & Betancourt, 1998), exemplifies how extreme climatic events may remove or suppress competitive limitations and promote invasion (White *et al.*, 2001). In this case, the drought provided a relatively short ‘window of opportunity’ for increased shrub growth and expansion.
- (iii) While our modeling results generally support the hypothesis that an increase in the number of large precipitation events could favor shrub establishment and growth, our results are somewhat equivocal. The key issues are (i) what constitutes a ‘large’ event and (ii) its timing (both *current* and *antecedent* conditions). Although we found that the soil water content (as measured by a synthetic index over time and both vertical/horizontal space) increased monotonically as rainfall was ‘redistributed’ into larger-size events while maintaining annual amounts and the summer to winter/spring ratios, the responses of the plants were highly nonlinear. The removal of the smallest events (<5 and <10 mm) tended to promote grass growth and suppress shrubs; in contrast, the removal of precipitation events <20 mm suppressed grasses but promoted shrub growth. The suite of complex factors governing the interactions between the timing and amount of rainfall, its subsequent effects on soil water content, and the

growth and reproduction of plants makes it difficult to make generalizations.

- (iv) The inclusion of spatially explicit runoff/run-on hydrologic flows provides valuable insight for testing hypotheses dealing with precipitation in rangelands. We found significant effects of runoff/run-on redistribution on both the plant and soil responses to seasonal shifts in precipitation, the effects of which depend on the functional characteristics of the plant, landscape position, and soil type.
- (v) Arid and semiarid rangelands are particularly vulnerable to climate variability, especially precipitation. A slight shift in the seasonal precipitation and/or the frequency of extreme events (e.g., the drought of the 1950s in the United States) could potentially lead to significant ecological and biogeochemical impacts, but these impacts will be influenced by local grazing history and management, current stocking rates, soil types, and species composition. These agents, especially grazing by domestic livestock, must be included in models in order to elucidate the relative importance of biotic vs. abiotic factors in historical grass–shrub dynamics in systems such as the Jornada Basin of southern New Mexico.

Acknowledgements

The authors thank John Anderson for his assistance in accessing the LTER data sets. Paul Kemp assisted in the development of the model and provided insightful comments on the manuscript. This research was supported by USDA Specific Cooperative Agreement #58-1270-3-070, the Center for Integrated Study of the Human Dimensions of Global Change (Carnegie Mellon University, SBR-9521914), the National Science Foundation of China Grants #90202008 and #90211002, the Chinese Ministry of Science and Technology Grant #2000018605, and is a contribution to the Jornada Basin LTER.

References

- Archer S (1999) Woody plant encroachment into southwestern grasslands and savannas: rates, patterns, and proximate causes. In: *Ecological Implications of Livestock Herbivory in the West* (ed. Pieper R), 2nd edn. pp. 13–68. Society for Range Management, Denver, Colorado.
- Bahre CJ, Shelton ML (1993) Historic vegetation change, mesquite increases, and climate in southeastern Arizona. *Journal of Biogeography*, 20, 489–504.
- Barbour MG (1968) Germination requirements of the desert shrub *Larrea divaricata*. *Ecology*, 915–923.
- Bennett WE, Mooney HA (1979) The water relations of some desert plants in Death Valley, California. *Flora*, 168, 405–427.
- Brown JH, Valone TJ, Curtin CG (1997) Reorganization of an arid ecosystem in response to recent climate change. *Proceedings of the National Academy of Sciences*, 94, 9729–9733.

- Brown JR, Archer S (1989) Woody plant invasion of grasslands: establishment of honey mesquite (*Prosopis glandulosa* var. *glandulosa*) on sites differing in herbaceous biomass and grazing history. *Oecologia*, 80, 19–26.
- Buffington LC, Herbel CH (1965) Vegetational changes on a semidesert grassland range from 1858 to 1963. *Ecological Monographs*, 35, 139–164.
- Burgess TL (1995) Desert grassland, mixed shrub savanna, shrub steppe, or semidesert scrub? The dilemma of coexisting growth forms. In: *The Desert Grassland* (eds McClaran MP, Van Devender TR), pp. 31–67. The University of Arizona Press, Tucson.
- Busch DE, Smith SD (1995) Mechanisms associated with decline of woody species in riparian ecosystems of the southwestern United States. *Ecological Monographs*, 65, 347–370.
- Bush JK, Van Auken OW (1987) Light requirements for growth of *Prosopis glandulosa* seedlings. *Southwestern Naturalist*, 32, 469–474.
- Bush JK, Van Auken OW (1990) Growth and survival of *Prosopis glandulosa* seedlings associated with shade and herbaceous competition. *Botanical Gazette*, 151, 234–239.
- Bush JK, Van Auken OW (1991) Importance of time of germination and soil depth on growth of *Prosopis glandulosa* (Leguminosae) seedlings in the presence of a C-4 grass. *American Journal of Botany*, 78, 1732–1739.
- Campbell GS, Jungbauer JD Jr, Shiozawa S *et al.* (1993) A one-parameter equation for water sorption isotherm of soils. *Soil Science*, 156, 302–306.
- Conley W, Conley MR, Karl TR (1992) A computational study of episodic events and historical context in long-term ecological process: climate and grazing in the northern Chihuahuan Desert. *Coenoses*, 7, 55–60.
- Cornelius JM, Kemp PR, Ludwig JA *et al.* (1991) The distribution of vascular plant species and guilds in space and time along a desert gradient. *Journal of Vegetation Science*, 2, 59–72.
- de Soyza AG, Franco AC, Virginia RA *et al.* (1996) Effects of plant size on photosynthesis and water relations in the desert shrub *Prosopis glandulosa* (Fabaceae). *American Journal of Botany*, 83, 99–105.
- Epstein HE, Burke IC, Lauenroth WK (1999) Response of the shortgrass steppe to changes in rainfall seasonality. *Ecosystems*, 2, 139–150.
- Fernández RJ, Reynolds JF (2000) Potential growth and drought tolerance of eight desert grasses: lack of a trade-off? *Oecologia*, 123, 90–98.
- Franco AC, de Soyza AG, Virginia RA *et al.* (1994) Effects of plant size and water relations on gas exchange and growth of the desert shrub, *Larrea tridentata*. *Oecologia*, 97, 171–178.
- Freudenberger DO, Hiernaux P (2001) Productivity of patterned vegetation. In: *Banded Vegetation Patterning in Arid and Semiarid Environments* (ed. Seghieri J), Ecological Studies Series, Vol. 149. pp. 198–209. Springer-Verlag, Berlin, New York, Heidelberg.
- Fulbright TE, Kuti JO, Tipton AR (1995) Effects of nurse-plant canopy temperatures on shrub seed germination and seedling growth. *Acta Oecologica – International Journal of Ecology*, 16, 621–632.
- Gao Q, Li JD, Zheng HY (1996) A dynamic landscape simulation model for the alkaline grasslands on Songnen Plain in northeast China. *Landscape Ecology*, 11, 339–349.
- Gibbens RP, Beck RF (1988) Changes in grass basal area and forb densities over a 64-year period on grassland types of the Jornada Experimental Range. *Journal of Range Management*, 41, 186–192.
- Gile LH, Hawley JW, Grossman RB, *et al.* (1988) 1988 Supplement to the Desert Project Guidebook. New Mexico Bureau of Mines and Mineral Resources, Socorro, New Mexico.
- Golluscio RA, Sala OE, Lauenroth WK (1998) Differential use of large summer rainfall events by shrubs and grasses: a manipulative experiment in the Patagonian steppe. *Oecologia*, 115, 17–25.
- Grover HD, Musick HB (1990) Shrubland encroachment in southern New Mexico, USA: an analysis of desertification processes in the American Southwest. *Climatic Change*, 17, 305–330.
- Guo Q, Rundel PW, Goodall DW (1998) Horizontal and vertical distribution of desert seed banks: patterns, causes and implications. *Journal of Arid Environments*, 39, 465–478.
- Guo QF, Rundel PW, Goodall DW (1999) Structure of desert seed banks: comparisons across four North American desert sites. *Journal of Arid Environments*, 42, 1–14.
- Herbel C, Dittberner P, Bickle TS (1970) In *Simulation and Analysis of Dynamics of a Semi-Desert Grassland: An Interdisciplinary Workshop Program Toward Evaluating the Potential Ecological Impact of Weather Modification* (ed. Van Dyne GM), pp. 133–178. Colorado State University, Fort Collins, CO.
- Huenneke LF, Anderson JP, Remmenga M *et al.* (2002) Desertification alters patterns of aboveground net primary production in Chihuahuan ecosystems. *Global Change Biology*, 8, 247–264.
- Kemp PR, Reynolds JF (2000) Variability in phenology and production of desert ephemerals: implications for predicting resource availability for desert tortoises. *Proceedings of the 24th Annual Meeting and Symposium of the Desert Tortoise Council*, pp. 34–39. St George, UT.
- Kemp PR, Reynolds JF, Ludwig JA (2003a) Effects of variation in rainfall, soil moisture, nitrogen availability, and landscape position on cover of plant functional types in the northern Chihuahuan Desert. *Journal of Vegetation Science* (in press).
- Kemp PR, Reynolds JF, Pachepsky Y *et al.* (1997) A comparative modeling study of soil water dynamics in a desert ecosystem. *Water Resources Research*, 33, 73–90.
- Kemp PR, Reynolds JF, Virginia RA *et al.* (2003b) Decomposition of leaf and root litter of Chihuahuan Desert shrubs: effects of three years of summer drought. *Journal of Arid Environments*, 53, 21–39.
- Kyparissis A, Grammatikopoulos G, Manetas Y (1997) Leaf demography and photosynthesis as affected by the environment in the drought semi-deciduous Mediterranean shrub *Phlomis fruticosa* L. *Acta Oecologica – International Journal of Ecology*, 18, 543–555.

- Lee SG, Felker P (1992) Influence of water/heat stress on flowering and fruiting of mesquite (*Prosopis glandulosa* var. *glandulosa*). *Journal of Arid Environments*, 23, 309–319.
- Lei SA (1997) Variation in germination response to temperature and water availability in blackbrush (*Coleogyne ramosissima*) and its ecological significance. *Great Basin Naturalist*, 57, 172–177.
- McAuliffe JR (1988) Markovian dynamics of simple and complex desert communities. *American Naturalist*, 131, 459–490.
- McPherson GR (1997) *Ecology and Management of North American Savannas*. University of Arizona Press, Tucson, AZ, USA.
- Monteith JL, Unsworth MH (1990) *Principles of Environmental Physics*. Edward Arnold, London.
- Naeth MA, Chanasyk DS (1996) Runoff and sediment yield under grazing in foothills fescue grasslands of Alberta. *Water Resources Bulletin*, 32, 89–95.
- Neilson RP (1986) High-resolution climatic analysis and southwest biogeography. *Science*, 232, 27–34.
- Ogle K, Reynolds JF (2002) Desert dogma revisited: coupling of stomatal conductance and photosynthesis in the desert shrub, *Larrea tridentata*. *Plant Cell and Environment*, 25, 909–922.
- Peters D (2002) Recruitment potential of two perennial grasses with different growth forms at a semiarid–arid transition zone. *American Journal of Botany*, 89, 1616–1623.
- Reynolds JF (1986) Adaptive strategies of desert shrubs with special reference to the creosotebush (*Larrea tridentata* [DC] Cov). In: *Pattern and Process in Desert Ecosystems* (ed. Whitford WG), pp. 19–49. University of New Mexico Press, Albuquerque, NM.
- Reynolds JF (2001) Desertification. In: *Encyclopedia of Biodiversity*, Vol. 2 (ed. Levin S), pp. 61–78. Academic Press, San Diego, CA.
- Reynolds JF, Cunningham GL (1981) Validation of a primary production model of the desert shrub *Larrea tridentata* using soil-moisture augmentation experiments. *Oecologia*, 51, 357–363.
- Reynolds JF, Fernández RJ, Kemp PR (2000a) Drylands and global change: rainfall variability and sustainable rangeland production. In: *Proceedings of the 12th Toyota Conference: Challenge of Plant and Agricultural Sciences to the Crisis of Biosphere on the Earth in the 21st Century* (ed. Komanine A), pp. 73–86. R.G. Landes Company, Austin, TX.
- Reynolds JF, Kemp PR, Tenhunen JD (2000b) Effects of long-term rainfall variability on evapotranspiration and soil water distribution in the Chihuahuan Desert: a modeling analysis. *Plant Ecology*, 150, 145–159.
- Reynolds JF, Stafford Smith DM (eds) (2002) *Global Desertification: Do Humans Cause Deserts?* Dahlem Workshop Report 88. Dahlem University Press, Berlin.
- Reynolds JF, Virginia RA, Kemp PR *et al.* (1999) Impact of drought on desert shrubs: effects of seasonality and degree of resource island development. *Ecological Monographs*, 69, 69–106.
- Reynolds JF, Virginia RA, Schlesinger WH (1997) Defining functional types for models of desertification. In: *Plant Functional Types: Their Relevance to Ecosystem Properties and Global Change* (ed. Woodward FI), pp. 194–214. Cambridge University Press, Cambridge, England.
- Schlesinger WH, Reynolds JF, Cunningham GL *et al.* (1990) Biological feedbacks in global desertification. *Science*, 247, 1043–1048.
- Schwinning S, Ehleringer J (2001) Water use trade-offs and optimal adaptations to pulse-driven arid ecosystems. *Journal of Ecology*, 89, 464–480.
- Sharpe PJH, Rykiel EJ Jr. (1991) Modelling integrated response of plants to multiple stresses. In: *Response of Plants to Multiple Stresses* (ed. Pell EJ), pp. 205–224. Academic Press, San Diego, CA.
- Swetnam TW, Betancourt JL (1998) Mesoscale disturbance and ecological response to decadal climatic variability in the American Southwest. *Journal of Climate*, 11, 3128–3147.
- Vaughton G (1998) Soil seed bank dynamics in the rare obligate seeding shrub, *Grevillea barklyana* (Proteaceae). *Australian Journal of Ecology*, 23, 375–384.
- Wainwright J, Mulligan M, Thornes J (1999) Plants and water in drylands. In: *Eco-hydrology: Plants and Water in Terrestrial and Aquatic Environments* (ed. Wilby RL), pp. 78–126. Routledge, London.
- Walter H (1971) Natural savannahs as a transition to the arid zone. In: *Ecology of Tropical and Subtropical Vegetation* (ed. Burnett JH), pp. 238–265. Van Nostrand Reinhold Co., New York.
- Weltz MA, Blackburn WH (1995) Water budget for south Texas rangelands. *Journal of Range Management*, 48, 45–52.
- White TA, Campbell BD, Kemp PD *et al.* (2001) Impacts of extreme climatic events on competition during grassland invasions. *Global Change Biology*, 7, 1–13.
- Wiegand T, Milton SJ, Wissel C (1995) A simulation model for a shrub ecosystem in the semiarid Karoo, South Africa. *Ecology*, 76, 2205–2221.
- Wierenga PJ, Hendrickx JMH, Nash MH *et al.* (1987) Variation of soil and vegetation with distance along a transect in the Chihuahuan Desert. *Journal of Arid Environments*, 13, 53–63.
- York JC, Dick-Peddie WA (1969) Vegetation changes in southern New Mexico during the past hundred years. In: *Arid Lands in Perspective* (ed. Goldman BJ), pp. 157–166. University of Arizona Press, Tucson, AZ.

Appendix A

The structure of MALS is presented here. MALS is a spatially explicit version of PALS, an ecosystem model that consists of modules for soil water, decomposition, energy-budget/atmospheric environment, and the physiology and phenology of the principal plant FTs of the southwestern United States (Reynolds *et al.*, 1997; Reynolds *et al.*, 2000b; Kemp *et al.*, 2003a).

The total dry weight (W_T) of each plant FT is partitioned into leaves (W_L), stem (W_S), root (W_R), and seeds (W_{seed}):

$$W_T = W_L + W_S + W_R + W_{seed}. \quad (A.1)$$

FTs are indicated by subscripts $i = 1$ (grass + herbs), 2 (evergreen shrubs, viz., *Larrea*), and 3 (deciduous shrubs, viz., *Prosopis*). We make several key assump-

tions in this version of MALS: (i) assimilated carbon (C) is available throughout the plant, ignoring short- vs. long-term transport; (ii) no distinction is made between labile and nonlabile C; and (iii) the effect of nutrients on assimilation and growth is ignored.

For brevity, explanations of all symbols, functions, and units are provided in Table A1.

A.1. Assimilation

The daily net assimilation (A) follows Reynolds *et al.* (1986):

$$A = \frac{g}{\Omega} \left(\frac{C_a - C_i}{P_a} \right) \beta \left(\frac{Y}{f_c} \right) Q(T_a) W_L SLA I_d. \quad (A.2)$$

Table A1 Symbols, functions, and units used in MALS

Eqn	Symbol	Definition	Units/value
1	W_L	Leaf dry weight	$g\ m^{-2}$
1	W_R	Root dry weight	$g\ m^{-2}$
1	W_S	Stem dry weight	$g\ m^{-2}$
1	W_{seed}	Seed dry weight	$g\ m^{-2}$
1	W_T	Total plant dry weight	$g\ m^{-2}$
2	β	Molecular mass of carbon (12)	$g\ mol^{-1}$
2	Ω	Ratio of H ₂ O to CO ₂ diffusion	1.6
2	d_{len}	Daylength = $12 + 2 \cos \left[2\pi \frac{t-172}{365.25} \right]$	h
2	f_c	Carbon fraction (0.5)	Dimensionless
2	g	Stomata conductance	$mol\ m^{-2}\ s^{-1}$
2	A	Assimilation rate	$g\ m^{-2}\ day^{-1}$
2	C_a	Partial pressure of CO ₂ in air	kPa
2	C_i	Partial pressure of CO ₂ in intercellular spaces	kPa
2	I_d	Daily integral = $3600 \frac{2}{\pi} d_{len}$ (Monteith & Unsworth 1990)	s
2	P_a	Atmospheric (barometric) pressure (= 0.88, Las Cruces, NM)	kPa
2	$Q(T_a)$	Effect of temperature on assimilation rate (0-1, see Eqn (15))	Dimensionless
2	SLA	Specific leaf area	$m^2\ g^{-1}$
2	T_a	Average daily air temperature	°C
2	Y	Yield or growth conversion efficiency	Dimensionless
3	ψ_i^{plant}	Plant water potential for the <i>i</i> th FT	MPa
3	a_i	Maximum stomatal conductance for the <i>i</i> th FT	$mol\ m^{-2}\ s^{-1}$
3	b_1	Stomatal conductance parameter for grasses	kPa^{-1}
3	b_2, b_3	Stomatal conductance parameter for shrubs	$mol\ m^{-2}\ s^{-1}\ kPa^{-1}$
3	c_i	Stomatal conductance parameter for shrubs	$mol\ m^{-2}\ s^{-1}\ kPa^{-1}$
3	VPD _{ave}	Average vapor pressure deficit	kPa
4	λ_{seed}	Proportion of assimilate allocated to seeds	Dimensionless
4	λ_{root}	Proportion of assimilate allocated to roots	Dimensionless
4	λ_{stem}	Proportion of assimilate allocated to stems	Dimensionless
4	λ_{leaf}	Proportion of assimilate allocated to leaves	Dimensionless
5	κ_{max}	Maximum proportional allocation to seeds	Dimensionless
5	a_s	Seed allocation parameter	MPa^{-1}
5	b_s	Seed allocation parameter	MPa
5	t	Julian day	day
5	$Q(t)$	Unimodal function for timing of seed phenology (0–1, see Eqn (15))	0–1
6	ρ_{root}	Proportional allocation to roots under nonlimiting conditions	Dimensionless
6	ϕ	Root allocation function	Dimensionless
6	S_ψ	Function for the effect of ψ_{plant} on root allocation	Dimensionless
7	ϕ	Stem allocation function (= $\rho_{stem}/(\rho_{leaf} + \rho_{stem})$)	Dimensionless
7	ρ_{leaf}	Parameter, proportional allocation to leaves under nonlimiting conditions	Dimensionless
7	ρ_{stem}	Parameter, proportional allocation to stems under nonlimiting conditions	Dimensionless
8	k_v	Seedling survivorship parameter	Dimensionless
8	F_{clay}	Clay content of soil (fraction)	Dimensionless
8	G_{max}	Maximum germination rate	day^{-1}
8	G_{seed}	Germination rate	day^{-1}

(continued)

Table A1 (Contd.)

Eqn	Symbol	Definition	Units/value
8	$Q(\text{SWC}_{15})$	Unimodal function for effect of soil water on seed germination (0–1, see Eqn (15))	Dimensionless
8	$Q(T_{\text{soil15}}^{\text{ave10}})$	Unimodal function for effect of temperature on seed germination (0–1, see Eqn (15))	Dimensionless
8	S_v	Seedling survivorship (fraction)	Dimensionless
8	$S_{v\text{max}}$	Maximum seedling survivorship	Dimensionless
8	SWC_{15}	Soil water content in upper 15 cm	cm
8	$T_{\text{soil15}}^{\text{ave10}}$	10-d average soil temperature at 15 cm depth	°C
9	ξ	Dummy variable for x	m
9	ζ	Dummy variable for y	m
9	σ_s	Standard deviation of seed dispersal	m
9	x	Horizontal coordinate	m
9	y	Horizontal coordinate	m
9	D_s	Seed dispersal function for shrub FTs	m^{-2}
10	Θ	Spatial domain of simulation	Dimensionless
10	d_{seed}	Natural senescence death rate of leaves	day^{-1}
11	α	Rhizome propagation coefficient	$\text{m}^2 \text{day}^{-1}$
11	λ_{realloc}	Reallocation coefficient	day^{-1}
11	d_{root}	Root senescence rate	day^{-1}
11	I_{phen}	Phenological trigger for reallocation in spring (0–1)	–
12	δ_{leaf}	Leaf death due to temperature stresses	Dimensionless
12	d_{leaf}	Leaf senescence rate	day^{-1}
12	d_{stem}	Stem senescence rate	day^{-1}
12	T_{min}	Minimum daily air temperature	°C
12	T_{Thres}	Threshold temperature for leaf loss	°C
12	U_T	Leaf death parameter	°C ⁻²
13	θ^j	Volumetric soil water content in soil layer j	$\text{cm}^{-3} \text{cm}^{-3}$
13	ΔZ^j	Thickness of soil layer j	cm
13	f_{in}^j	Flow of water into soil layer j	cm day^{-1}
13	f_{out}^j	Flow of water out of soil layer j	cm day^{-1}
13	$f_{(j-1)j}$	Vertical from layer $(j-1)$ to layer j	cm day^{-1}
13	Δt	Time increment	day
13	E	Soil evaporation	cm day^{-1}
13	P	Effective daily precipitation	cm day^{-1}
13	R_{off}	Daily surface runoff	cm day^{-1}
13	R_{on}	Daily surface run-on	cm day^{-1}
13	T_r^j	Transpiration water loss from soil layer j	cm day^{-1}
14	z_j	Vertical coordinates, elevation	m
15	u	Independent variable	
15	u_1, u_2, u_3, u_4	Dependent variables	
15	Q	Q functions	Dimensionless
20	θ_f^j	Field capacity, in terms of volumetric water content	$\text{cm}^{-3} \text{cm}^{-3}$

The equation where symbols first appear is noted. The three plant FTs (grass + herbs, evergreen shrubs, and deciduous shrubs) are indicated by subscript $i = 1, 2,$ and $3,$ respectively.

The effect of the average daily air temperature (T_a) on assimilation is described by a scalar (Q function, see Section A.6), whereas stomata conductance (g) is assumed to increase with the plant water potential (ψ^{plant}) and decrease with the vapor pressure deficit (VPD) (Reynolds *et al.*, 1999; Franco *et al.*, 1994). Stomata conductance in the shrub FTs is assumed to increase linearly with increasing ψ^{plant} , whereas in

grass + herbs FT it increases exponentially:

$$g_i = \begin{cases} a_i \exp(b_i \psi_i^{\text{plant}}) [1 - 0.1 \text{VPD}_{\text{ave}}] & \text{for } i = 1, \\ a_i + b_i \psi_i^{\text{plant}} - c_i \text{VPD}_{\text{ave}} & \text{for } i = 2, 3, \end{cases} \quad (\text{A.3})$$

where ψ^{plant} is computed from the average soil water potential over three soil layers (see Section A.4),

weighed by root fractions of each FT in each soil layer (details in Kemp *et al.*, 1997).

A.2. Allocation

Newly assimilated products (A) are proportionally allocated to leaves (λ_{leaf}), stems (λ_{stem}), roots (λ_{root}), and seeds (λ_{seed}), i.e.

$$1 = \lambda_{leaf} + \lambda_{stem} + \lambda_{root} + \lambda_{seed}. \quad (A.4)$$

Allocation to seeds and roots is given by

$$\lambda_{seed} = \kappa_{max} Q(t) \exp[-a_s (b_s + \psi^{plant})], \quad (A.5)$$

$$\lambda_{root} = \phi (1 - \lambda_{seed}), \quad (A.6a)$$

where

$$\phi = \frac{4 \rho_{root}}{3 + S_\psi}, \quad (A.6b)$$

$$S_\psi = \begin{cases} \exp[0.2(\psi^{plant} + 1.5)] & \text{if } \psi^{plant} < -1.5 \text{ MPa,} \\ 1 & \text{otherwise.} \end{cases} \quad (A.6c)$$

This allocation scheme is based on Reynolds *et al.* (1986) and Sharpe & Rykiel (1991), where S_ψ describes the dependence of allocation on ψ^{plant} . As ψ^{plant} decreases from -1.5 MPa (i.e., increasing water stress), S_ψ decreases from 1 to 0, resulting in a greater allocation of assimilated products to roots. Allocation to seeds (Eqn (A.5)) is assumed to be a function of phenology (time) and ψ^{plant} , where κ_{max} is the maximum proportion of A allocated to seeds and the scalar $Q(t)$ controls its timing (i.e., phenology). Eqn (A.5) is parameterized such that a greater proportion of assimilated products is allocated to seeds with increasing water stress (Reynolds & Cunningham, 1981; Lee & Felker, 1992). Only adult shrubs produce seeds.

Allocations to stems (λ_{stem}) and leaves (λ_{leaf}) are given by

$$\lambda_{stem} = \varphi (1 - \phi) (1 - \lambda_{seed}), \quad (A.7a)$$

$$\lambda_{leaf} = (1 - \varphi) (1 - \phi) (1 - \lambda_{seed}), \quad (A.7b)$$

where

$$\varphi = \rho_{stem} / (\rho_{stem} + \rho_{leaf}). \quad (A.7c)$$

A.3. Seed germination and dispersal

Seed germination is considered to be a unimodal function of the 10-day average surface soil temperature and topsoil water content. With regard to the grass + herbs FT, recruitment processes in C4 desert grasses are

not well understood and not readily explained by energetic models or life history traits (Peters, 2002). Because of the general lack of data for all species, and the study by Peters (2002), who reported that inflorescences in *B. eriopoda* often become rooted in the soil and thus function as stolons allowing this species to spread rapidly, we ignore sexual reproduction and assume that stolon production is the major means of propagation.

The seed germination rate (G_{seed} , day^{-1}) for both shrub FTs is determined by a maximum rate (G_{max}) scaled by the 10-day average soil temperature (T_{soil15}^{ave10}) and soil water content (SWC₁₅) in the upper 15 cm of the soil:

$$G_{Seed} = G_{max} Q(T_{soil15}^{ave10}) Q(SWC_{15}). \quad (A.8a)$$

By varying the shape and center of these Q functions, we were able to vary the sensitivities of germination to temperature and soil water (Kemp & Reynolds, 2000). The survivorship (S_v) in *Larrea* is assumed to be a function of the clay content of soil (F_{clay}) and a maximum survivorship rate (S_{vmax}), i.e.,

$$S_v = S_{vmax} \exp(-k_v F_{clay}), \quad (A.8b)$$

whereas the survivorship in *Prosopis* is assumed to be constant (Barbour, 1968; Brown & Archer, 1989; Fulbright *et al.*, 1995; Lei, 1997).

The spatial propagation in the two shrub FTs occurs via seed dispersal. Seed produced at a given location (ξ, ζ) in a two-dimensional landscape is assumed to disperse symmetrically around this point, following a Gaussian distribution centered at (ξ, ζ) (Guo *et al.*, 1998, 1999; Vaughton, 1998). Hence, $D_s(\xi - x, \zeta - y)$ is the proportion of seed produced at position (ξ, ζ) transported to position (x, y):

$$D_s(\xi - x, \zeta - y) = \frac{1}{2\pi(\sigma_s)^2} \exp\left(-\frac{1}{2} \left(\frac{(\xi - x)^2 + (\zeta - y)^2}{(\sigma_s)^2}\right)\right), \quad (A.9)$$

where σ_s is the variance of seed distribution specific to the shrub FTs. For the grass + herbs FT, we neglect sexual reproduction and assume only clonal growth via rhizomes.

A.4. Biomass dynamics

A.4.1. Seeds

Seed biomass dynamics is given by

$$\frac{\partial W_{seed}}{\partial t} = \int_{\theta} A \lambda_{seed}(\zeta, \xi) D_s(\xi - x, \zeta - y) d\xi d\zeta - (G_{seed} + d_{seed}) W_{seed}, \quad (A.10)$$

where Θ is the dispersal range, which is theoretically the domain of the simulation.

A.4.2. Roots

To simulate resprouting in the spring and early summer, there is a reallocation of biomass from roots to leaves, which is triggered by a phenology queue (I_{phen}); this re-allocation is assumed to be a constant fraction ($\lambda_{realloc}$). For the grass + herbs FT ($i = 1$), rhizome propagation is assumed to be proportional to the gradient of the root biomass. Hence, the dynamics of the root biomass for FT i ($W_{R,i}$) is given by

$$\frac{\partial W_{R,i}}{\partial t} = \begin{cases} A \lambda_{root} - \lambda_{realloc} W_{R,i} I_{phen} - d_{root} W_{R,i} + \alpha \left(\frac{\partial^2 W_{R,i}}{\partial x^2} + \frac{\partial^2 W_{R,i}}{\partial y^2} \right) & \text{for } i = 1, \\ A \lambda_{root} + \phi [S_v G_{seed} W_{seed}] - \lambda_{realloc} W_{R,i} I_{phen} - d_{root} W_{R,i} & \text{for } i = 2, 3, \end{cases} \quad (A.11)$$

where α is the rhizome propagation coefficient. In this version of the model, rhizome propagation is one dimensional, i.e., between neighboring 10 m × 30 m cells along the transect. Note that the second term in Eqn (A.11) for the shrub FTs ($i = 2,3$) represents the proportion of the new biomass allocated to roots from germinating seeds.

A.4.3. Leaves and stems

The dynamics of leaf and stem biomass are given by

$$\frac{\partial W_L}{\partial t} = \lambda_{leaf} \left[A + \frac{S_v G_{seed} W_{seed}}{(1 - \lambda_{seed})} \right] + I_{phen} \lambda_{realloc} (W_R + W_S) - d_{leaf} (1 + \delta_{leaf}) W_L, \quad (A.12a)$$

$$\frac{\partial W_S}{\partial t} = \lambda_{stem} \left[A + \frac{S_v G_{seed} W_{seed}}{(1 - \lambda_{seed})} \right] - I_{phen} \lambda_{realloc} W_S - d_{stem} W_S, \quad (A.12b)$$

where δ_{leaf} represents the accelerated death rates over natural senescence (i.e., d_{leaf}) in leaves due to temperature stress. While senescence is assumed to be constant, loss due to temperature stress is given by a threshold function

$$\delta_{leaf} = \begin{cases} 0 & \text{if } T_{min} > T_{Thres}, \\ U_T (T_{min} - T_{Thres})^2 & \text{if } -6 \leq T_{min} < T_{Thres}, \\ U_T (-6.0 - T_{Thres})^2 & \text{otherwise,} \end{cases} \quad (A.12c)$$

where U_T and T_{Thres} are parameters specific to each FT (Bennert & Mooney, 1979; Busch & Smith, 1995; Kyparissis *et al.*, 1997).

A.5. Soil water dynamics

The spatial and temporal variation of soil water is affected by precipitation (P), evaporation at surface soil (E), plant transpiration (T_r), and surface runoff (R_{off}) and run-on (R_{on}). Soil water is lost by evaporation (top and middle layers) and plant transpiration (all three layers). The effect of evapotranspiration follows Campbell *et al.* (1993). The vertical soil water movement between soil layers is modeled following the algorithm in Kemp *et al.* (1997). Because of the relatively low matrix potentials and resultant low hydraulic conductivities that exist during most of the year at 60 and 90 cm depths, the redistribution of water in the soil profile is very slow as compared to water extraction by roots and evaporation, and is treated in a very simple manner in our model as described in Kemp *et al.* (1997). Calculations of soil water retention characteristics, evaporation from soil surface, transpiration by plants, and soil temperature are given in Kemp *et al.* (1997) and Reynolds *et al.* (2000b). The soil water potential, field capacity, and minimum soil water contents, were calculated as functions of soil clay contents following Campbell *et al.* (1993). A brief overview of the soil model is presented below.

The soil is divided into three layers: 0–15, 15–40, and 40–80 cm. The bottom layer (80 cm) is assumed to represent an impregnable caliche deposition layer, i.e., at this depth, water loss is via root uptake only as detailed in Kemp *et al.* (1997). The water content of each layer is modeled as

$$\frac{d\theta^j}{dt} = \frac{1}{\Delta Z^j} (f_{in}^j - f_{out}^j), \quad (A.13a)$$

where θ^j is the volumetric soil water content, ΔZ^j is the thickness of the layer, and f_{in}^j and f_{out}^j are flows into and out of layer j :

$$f_{in}^j = \begin{cases} P - E + R_{on} - R_{off} & \text{for } j = 1, \\ f_{(j-1)j} & \text{for } j = 2, 3, \end{cases} \quad (A.13b)$$

$$f_{out}^j = f_{j(j+1)} + T_r^j \quad \text{for } j = 1, 2, 3, \quad (A.13d)$$

where $f_{j(j+1)}$ is the vertical flow from soil layer j to layer $j + 1$, and T_r^j is the transpiration water loss from soil layer j . The interlayer flow $f_{j(j+1)}$ is given by

$$f_{j(j+1)} = \begin{cases} f_{in}^j - T_r^j + \frac{\Delta Z^j (\theta^j - \theta_{f}^j)}{\Delta t} & \text{if } \frac{\Delta t}{\Delta Z^j} (f_{in}^j - T_r^j) + \theta^j > \theta_{f}^j, \\ 0 & \text{otherwise,} \end{cases} \quad (A.13e)$$

where θ_{f}^j is the field capacity of layer j and $\Delta t = 1$ day. Hence, the water flow between layers is only possible if the upper soil layer reaches field capacity. The three plant FTs are assumed to have different rooting patterns in the three soil layers following the approach of Kemp *et al.* (1997). A threshold value of the total plant biomass

(W_T) is assumed to differentiate between ‘young’ and ‘adult’ shrubs following Reynolds *et al.* (1999).

Runoff is produced when the total rainfall exceeds the infiltration rate and the surface soil is saturated. While the rate of infiltration and the maximum depth of percolation in soils depend on various factors, e.g., texture and plant root distributions, our treatment is highly simplified. We assume that the maximum depth of infiltration in a single day is 80 cm. The assumption is based on field observations by Reynolds *et al.* (1999), who reported that the wetting front along the transect reached a maximum of 0.6 m in 1991, a relatively wet year. Because our treatment of the soil water movement does not allow vertical redistribution, 0.8 m is set to be the maximum depth of penetration. Runoff from a grid cell in a discrete landscape domain (two dimensional) is distributed to one or more of its four neighboring cells having a lower elevation, and the relative allocation among neighborhood cells is assumed to be proportional to the steepness of the slope (Weltz & Blackburn, 1995; Naeth & Chanasyk, 1996; Kemp *et al.*, 1997), i.e.

$$R_{on}(i \rightarrow j) = R_{off}(i) \frac{\max(z_i - z_j, 0)}{\sum_{k=1}^4 \max(z_i - z_k, 0)}, \quad (A.14)$$

where $R_{off}(i)$ is the runoff produced at grid cell i , and $R_{on}(i \rightarrow j)$ is the run-on flow from grid cell i to one of its four neighbors j . The runoff produced at a boundary

grid cell is removed from the system if the cell has a lower elevation than its neighboring cells. An algorithm was designed in the model program to calculate the ultimate runoff and run-on flows for each day at each grid cell.

A.6. Q functions

All Q functions vary from 0 to 1 as follows:

$$Q(u) = Q(u_1, u_2, u_3, u_4, u) = \begin{cases} 0 & \text{if } u < u_1, \\ 2 \left(\frac{u-u_1}{u_2-u_1} \right)^2 & \text{if } u_1 \leq u < \frac{1}{2}(u_1 + u_2) \\ 1 - 2 \left(\frac{u_2-u}{u_2-u_1} \right)^2 & \text{if } \frac{1}{2}(u_1 + u_2) \leq u < u_2, \\ 1 & \text{if } u_2 \leq u < u_3, \\ 1 - 2 \left(\frac{u-u_3}{u_4-u_3} \right)^2 & \text{if } u_3 \leq u < \frac{1}{2}(u_3 + u_4), \\ 2 \left(\frac{u_4-u}{u_4-u_3} \right)^2 & \text{if } \frac{1}{2}(u_3 + u_4) \leq u < u_4 \\ 0 & \text{if } u \geq u_4, \end{cases} \quad (A.15)$$

This is a piecewise quadratic function with one peak value (1) and a continuous first derivative with respect to u . By varying the four parameters ($u_i, i = 1, 2, \dots, 4$), it can be used to approximate various symmetric or asymmetric unimodal functions (Gao *et al.*, 1996).